Extending first principles modeling with crystal chemistry: a bond-valence based classical potential

Valentino R. Cooper*, Ilya Grinberg* and Andrew M. Rappe*

*Department of Chemistry and Laboratory for Research on the Structure of Matter, University of Pennsylvania, Philadelphia, PA 19104-6323

Abstract. We demonstrate how a phenomenological model which reproduces first-principles density functional theory (DFT) calculations can be constructed to study complex ferroelectric oxides. This model is derived from a well-known crystal chemistry approach, in which Brown's Rules of Valence[1, 2] are used to determine the configurational energy of the system. Our previous work has shown that this model can be used to explain the atomic interactions in the $Pb(Zr_{1-x}Ti_x)O_3$ (PZT) solid solution. We extend this model by parameterizing to a distorted DFT structure as well as a structural minimum. Finally, we shall comment on the applicability of this model for finite-temperature and composition-dependent studies.

INTRODUCTION

A wide variety of complex oxides are used as ferroelectric materials in modern technology. These materials, usually in the perovskite form, have been found favorable for many applications, such as ultrasound machines, cell phones, radios and even Naval SONAR devices. In order to improve upon or propose new materials for use in these applications, it is necessary to understand the inter-atomic interactions in these systems. Density functional theory (DFT)[3] and other *ab initio* techniques have been proven to be effective in determining the local structural properties of many of these materials. However, like many other probes, DFT has its limitations. Due to the computational demands of DFT, it is not possible to use DFT to model large supercells. This makes it difficult to study disordered materials or materials with extensive long range correlated fluctuations. This also inhibits the ability to use DFT to observe phenomena such as domain wall shifting, ion transport, and doping and vacancy effects. In addition, DFT is a zero temperature probe making it difficult to extract finite temperature properties from these calculations.

In this regard, extensive research has been performed in developing DFT based models for studying finite temperature properties of large ferroelectric systems [4, 5, 6, 7]. It has been shown that such methods can be used to perform molecular dynamics and Monte Carlo simulations to predict temperature dependent phase transitions in oxides and to calculate phonon mode spectra. However, it is not always easy to use these methods to effectively study these systems, as they often have a large number of parameters which require fine tuning before they can be used in practice.

CP677, *Fundamental Physics of Ferroelectrics 2003*, edited by P. K. Davies and D. J. Singh

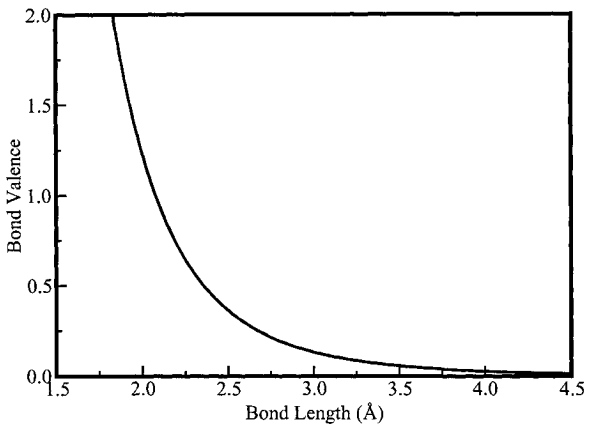

FIGURE 1. This plot depicts the bond-valence relation for a diatomic molecule. Here we see that the partial valence (or bond strength) contribution for each atom will increase with an inverse power law as the two atoms move closer to each other.

THE BOND VALENCE THEORY

For years, crystal chemists have used the bond-valence theory to assess the validity of various chemical structures. The bond-valence theory relates the bond strength (or valence) of an ionic pair to the inter-atomic distance (Figure 1). When the ions are sufficiently separated, there is no bonding interaction between them. As they move closer to each other there is an inverse power relation between the bond-strength and the bond distance (Equation 1).

$$s_{ij} = \left(\frac{R_{ij}}{R_0}\right)^{-N_{ij}} \tag{1}$$

Here R_{ij} is the distance between the two ions, R_0 is the length of a bond that would give a valence of 1, and N determines the rate of decay of the bonding interaction between the ith and jth ions. In a crystal structure, each ion will make bonding interactions such that the sum of all its bond-valences is equal to its nominal valence.

Figure 2 shows a valence map for a single Ti ion in the xy plane of on oxygen octahedron. If the Ti ion moves too close to a single oxygen ion there will be a dramatic increase in the ion's valence. In this configuration, the Ti ion will be over-bonded. Similarly, if the Ti ion remains in the center of the O octahedron, it will be under-bonded and the Ti ion will have to off-center to obtain its nominal valence of 4. Brown *et al.*[1, 2] have shown that the bond-valence theory corresponds remarkably with experimental data.

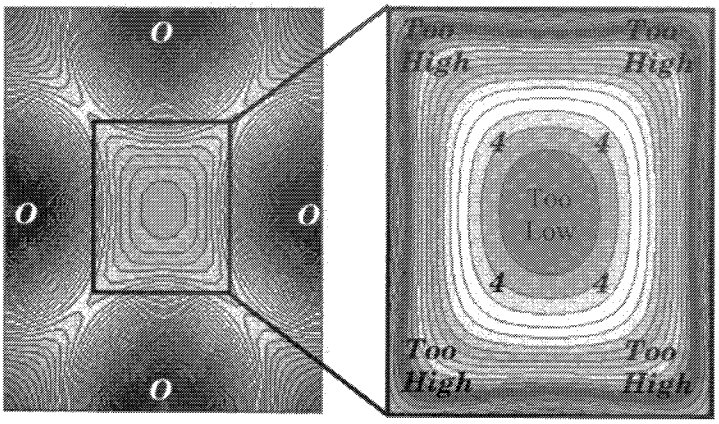

FIGURE 2. Valence of a single Ti ion as it moves in the x-y plane of its oxygen octahedron. As the Ti ion moves close to a single O ion there is an increase in the valence of the Ti ion and the Ti ion is said to be over-bonded. Conversely, if the Ti ion remains in the center of its oxygen octahedra it will be under-bonded as its valence would be significantly less than its nominal valence of 4.

PRACTICAL APPLICATIONS OF THE BOND VALENCE THEORY

Bond-valence arguments are used by X-ray crystallographers to eliminate chemically unreasonable structures and to give more credence to proposed structure[8, 9, 10]. In these approaches, the bond-valence analogy is further applied to identifying the valence states of the elements involved in the oxides studied.

Recently, theorists have begun to employ methods based on the bond-valence concept to model various chemical systems. Eck and co-workers have shown how an empirical potential based on the bond-valence concept, and parameterized from experimental data, can be used to effectively simulate solid systems[11]. They have extended this concept to molecular dynamics simulations (MD), extracting finite-temperature, physical and chemical information (such as structures, energetics, mobilities and reactivities) for an array of compounds[12]. These compounds include ionic/covalent solids, ternary compounds, metals and alloys.

Adams and Swenson have used a combination of bond-valence concepts and Reverse Monte Carlo (RMC) methods to investigate the migration pathways in Ag-based superionic glasses[13, 14]. They employ a bond valence potential (parameterized from experimental data) to evaluate the energy of structures produced by RMC techniques performed on experimental data.

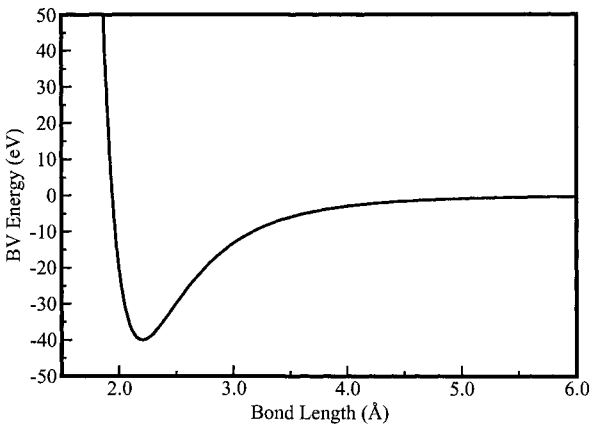

FIGURE 3. This plot shows the bond-valence energy dependence on distance for a diatomic molecule, as defined in our BV model. The bond-valence concept has been modified to assign an energy cost to each atom's inability to obtain its desired valence.

OUR MODIFIED BOND VALENCE MODEL

Bond-valence arguments can correctly predict which crystal structures are favored. However, we find that this concept alone cannot model structural distortions in complex ionic crystals. Therefore, we proceed to construct a potential which reflects each atom's desire to fulfill its bond valence. We augment this potential with other physically-motivated terms, so that the resulting potential is versatile enough to accurately reproduce DFT data for a wide variety of structures.

Our method, similar to the above mentioned studies, extends the bond-valence concept by assigning an energy cost to an atom's inability to achieve its desired valence. Our Bond-Valence (BV) model proposes the idea that in a relaxed structure each atom wants to achieve its desired valence by surrounding itself with the appropriate number of bonds. From this the energy due to the bond-valence interactions can be computed:

$$E_{\mathrm{BV}} = \sum_i A_i \left[\left| V_i - V_i^0 \right|^{\alpha_i} - V_i^{\alpha_i} \right], \tag{2}$$

Here V_i is the actual valence of the ith ion and V_i^0 is the nominal valence of that ion. A_i and α_i affect the total energy and the forces of the ion and are necessary for matching the BV forces and energies to density functional energies. Figure 3 shows the form of the bond valence potential.

One shortcoming of the bond-valence theory is that it does not include long-range electrostatic interactions, which play an important role in ionic systems such as the ferroelectric perovskites. To account for this we use an Ewald summation (E_{ewald}) to calculate the long range, Coulombic interactions. An additional short-range repulsive term (E_{rep}) is included (Equation 3) to prevent unphysically short distances which arise when only the Ewald and BV terms are used.

$$E_{\text{rep}} = \sum_{ij} A_{ij} \left[e^{-B_{ij} R_{ij}} \right] \tag{3}$$

The BV Model in Practice

Previously, we have shown that our BV model can be used to describe the local structure of the $Pb(Zr_{1-x}Ti_x)O_3$ (PZT) solid solution[15]. Figures 4 and 5 show the displacement patterns obtained from DFT and BV model calculations on a $4\times2\times1$ structure. The model gives good agreement with DFT minimum energy structures on small $4\times2\times1$ supercells. To compare these results to experimental data, we compute the pair distribution function (PDF) of the system. The PDF reveals the inter-atomic distances within a material. It is constructed from the Fourier transform of data obtained from pulsed neutron scattering experiments. The peak widths in an experimental PDF are related to both the thermal motion of the ions and the ionic disorder in the material. Figure 6 depicts the experimental PDF for the 50/50 monoclinic phase of PZT[16] and the PDFs obtained for a 40-atom DFT and a 320-atom BV model 50/50 monoclinic supercell calculation. The experimental results were obtained at 10K, thus limiting the effects of thermal motion within the material. The widths of the peaks show the extensive structural disorder within PZT.

The narrow peaks of the DFT PDF show that the DFT supercell is too small and ordered to explain the experimental PDF. In particular, the extra peaks at 4 Å and 8 Å are a result of the periodicity of the unit cell. The BV model has the advantage of being able to model larger, more disordered supercells. This can be seen through the excellent agreement of the 50/50 monoclinic experimental PDF with the PDF obtained from the 320

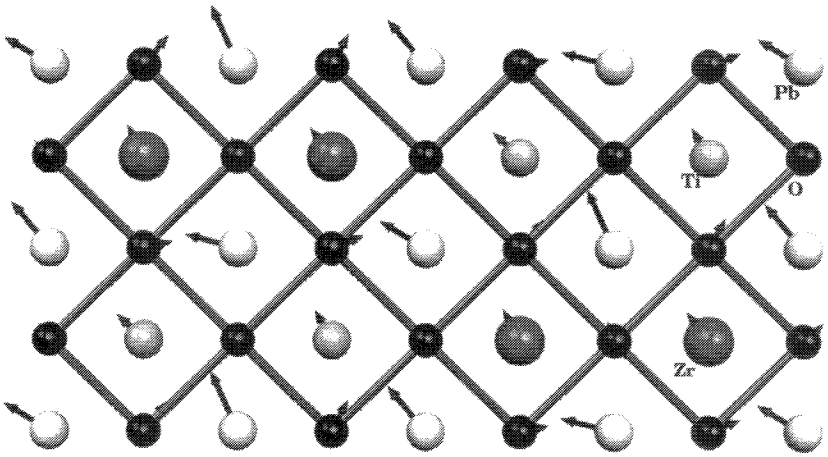

FIGURE 4. Projection of the $4\times2\times1$ 50/50 supercell DFT PZT structure onto the x-y plane. The oxygen octahedra are depicted by diamonds, and the distortions from the ideal cubic perovskite positions are shown by arrows. Pb atoms are 1/2 unit cell above the plane and apical O atoms are omitted.

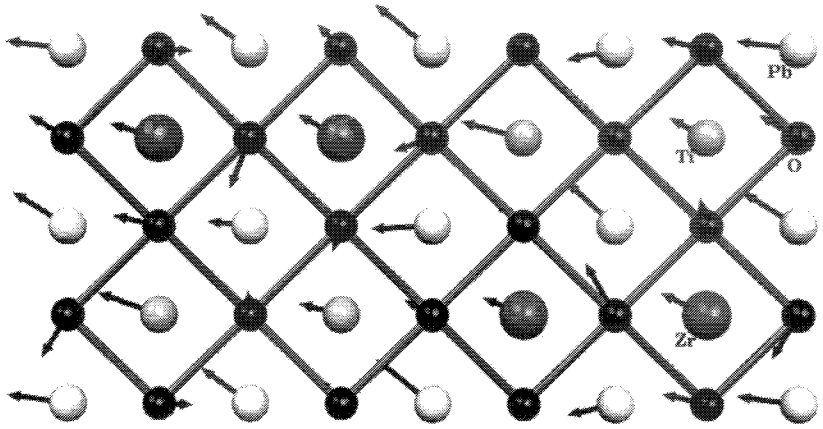

FIGURE 5. BV distortion pattern for structure shown in figure 4

atom BV supercell. Similar agreement was observed for both the 40/60 tetragonal and 60/40 rhombohedral phases. The fact that the tetragonal and rhombohedral supercells were all parameterized from the $4\times2\times1$ monoclinic PZT data points to the transferability of the BV model.

The BV model can be further applied as an analytical tool to explain the off-centering of the ions in PZT by comparing the valences and bond distances of Ti and Zr ions when structurally relaxed versus that of the ideal perovskite cube. Table 1 shows the partial valence and the nearest oxygen neighbor bond lengths for Ti in both the relaxed

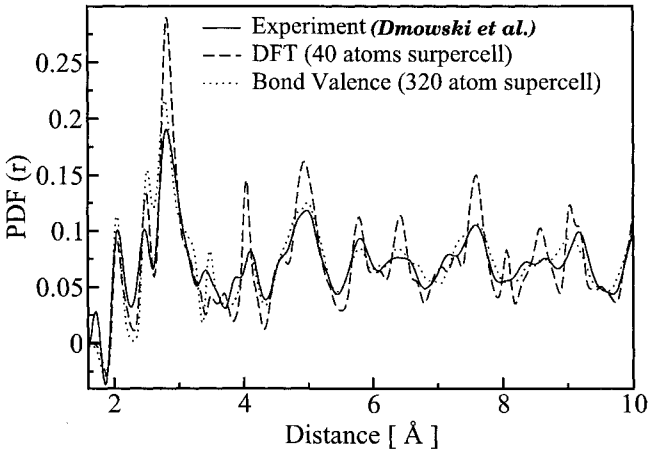

FIGURE 6. PDFs for 50/50 monoclinic PZT. Data are from experiment[16], DFT, and the BV model. Similar agreement with experiment was obtained with the BV model for the tetragonal and rhombohedral phases of PZT.

TABLE 1. Ti ion valence in ideal and DFT relaxed structures

Ti-O Bond Length	Ti Partial* Valence	Ti-O Bond Length	Ti Partial† Valence
2.015	0.631	1.822	1.071
2.015	0.631	2.358	0.279
2.015	0.631	1.939	0.775
2.015	0.631	2.027	0.614
2.070	0.549	1.999	0.660
2.070	0.549	2.067	0.555
Total	3.622	Total	3.954

* ideal perovskite structure
† DFT relaxed structure

and ideal perovskite structures for a $4\times2\times1$ DFT supercell. If the Ti ion remains in the center of the perfect perovskite structure it will be under-bonded with a valence of 3.622. To compensate for this under-bonding, the Ti ion off-centers to make one short Ti-O bond and one long bond, keeping the other bond distances relatively unchanged, and producing a more favorable Ti valence of 3.954.

Table 2 shows similar data for the interaction of the Zr ion with its oxygen octahedron. In this scenario, the ideal perovskite arrangement of this ion results in the Zr ion being over-bonded, with a total valence of 4.499. This is because the Zr ion is larger than the Ti ion and will interact more with its neighboring oxygen ions. In order to obtain its nominal valence, the Zr octahedron expands significantly, accompanied by a small Zr off-centering and octahedral rotation. This create three shorter Zr-O bonds and three longer ones, reducing the Zr valence to 3.996.

TABLE 2. Zr ion valence in ideal and DFT relaxed structures

Zr-O Bond Length	Zr Partial* Valence	Zr-O Bond Length	Zr Partial† Valence
2.015	0.789	1.984	0.865
2.015	0.789	2.214	0.449
2.015	0.789	2.028	0.759
2.015	0.671	2.086	0.641
2.070	0.671	2.058	0.696
2.070	0.789	2.118	0.586
Total	4.499	Total	3.996

* ideal perovskite structure
† DFT relaxed structure

SECOND GENERATION BOND VALENCE MODEL

Our first generation BV model (described above) gives excellent agreement with minimum energy DFT structures. It is able to reproduce the DFT displacement patterns in the relaxed structures, making it suitable for explaining minimum energy structure phenomena such as low temperature PDFs. However, in order to extend the use of the BV model to investigate finite temperature properties, it is necessary to parameterize our BV model using forces and energies from a database of DFT structures, including structures far from equilibrium.

Before BV parameters can be optimized, two things must be considered. First, a suitable database of structures must be constructed using DFT, from which to match forces and energies. Second, an efficient minimization routine must be chosen to automate the fine tuning of the BV parameters.

Constructing a Database of DFT Structures

We have constructed a database of 1000+ DFT PZT structures for the parameterization of the BV model. This database consists of 30 minimum energy structures, numerous structures obtained during the ionic relaxation steps used to determine the minimum energy structures, and structures resulting from further calculations in which a single atom was moved up to 0.8 Å in each direction from its DFT relaxed structure positions. The database contains a variety of cation arrangements and appropriately contains structures with forces up to 2 eV/Å on a single ion in a particular direction. High force structures are necessary to insure the accurate modeling of high-energy modes that may arise during molecular dynamics simulations.

Simulated Annealing: An Optimization Routine

In an attempt to optimize the BV parameters to produce the best quantitative agreement with DFT data, a simulated annealing[17] method was employed. In our implementation of simulated annealing, each of the BV parameters is randomly adjusted to make a trial step. Next, a penalty function is evaluated, based solely on the difference in the forces on the atoms obtained from the BV and the DFT calculations. Finally, the Metropolis Monte Carlo[18] algorithm is used to either accept or reject the proposed move. These steps are repeated for a selected number of moves after which the temperature is decreased.

This minimization routine is analogous to the cooling of a liquid. At high "temperatures" the parameters being minimized are allowed to change freely with respect to each other. As the temperature is reduced slowly, each parameter will adjust so as to settle into its preferred minimum configuration. This allows the routine to find a global minimum.

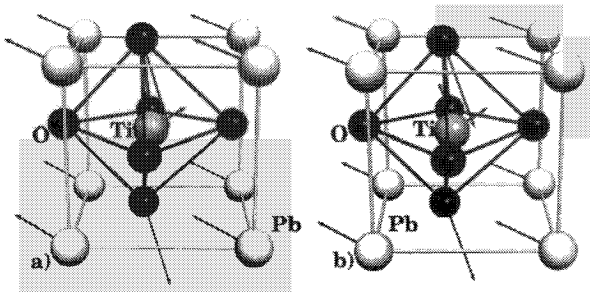

FIGURE 7. Optimized BV parameters are able to accurately reproduce DFT(a) forces (portrayed as arrows) on a high-energy test structure. The parameters obtained from the BV optimization routine give BV forces (b) that agree with DFT forces within an average deviation of 0.032 eV/Å per coordinate.

Preliminary Results: Lead Titanate ($PbTiO_3$)

Lead Titanate (PT) was used as a model system to test the effectiveness of the BV parameter optimization routine. PT has been extensively studied both theoretically and experimentally. It has a simple tetragonally distorted five-atom unit cell. Comparison of BV PT results with previous studies will give an indication as to the accuracy of both the fitting routine and the BV model for use in MD simulations.

For our initial investigations, BV parameters were optimized with two DFT structures. The first DFT structure was a high-energy structure, with ionic positions close to the ideal perovskite positions. The second structure was obtained from the ionic relaxation of the high-energy structure.

Preliminary results show that the current minimization routine is able to optimize parameters to an average deviation from DFT of 0.032 eV/Å per coordinate. Figure 7 depicts the forces on each ion in the high-energy structure obtained using DFT and the optimized BV parameters. Table 3 shows the actual forces on each atom in the high energy structure. Considering both Figure 7 and Table 3, we see that there is excellent agreement between the BV forces and the DFT forces. Furthermore, our DFT calculations report a cohesive energy of 38.45 eV/cell for the test PT structure. The BV structure is in good agreement with these results producing a cohesive energy of 39.62 eV/cell. These results give us confidence that the optimized BV parameters will be able to accurately reproduce DFT results and can be further applied to MD simulations to observe finite-temperature properties of complex oxide materials.

CONCLUSION

BV arguments have been used extensively by X-ray crystallographers to characterize the structure of many materials. Theoretical investigations have shown how these concepts can be used to construct a potential which can be used to explain experimental data such as PDFs of three different phases of PZT. While experimentally determined BV parameters give excellent qualitative agreement with accurate DFT calculations, fine tuning the

TABLE 3. DFT and Optimized Bond Valence Forces on atoms for a High Energy Structure of $PbTiO_3$

Species	x (eV/Å)	y (eV/Å)	z (eV/Å)
Pb(DFT)	-0.97	0.25	-0.59
Pb(BV)	-0.97	0.32	-0.58
Ti(DFT)	0.59	0.29	-0.38
Ti(BV)	0.57	0.28	-0.39
O_1(DFT)	-0.17	0.74	0.93
O_1(BV)	-0.11	0.73	0.88
O_2(DFT)	0.54	-1.49	0.22
O_2(BV)	0.48	-1.54	0.27
O_3(DFT)	0.01	0.21	-0.18
O_3(BV)	-0.02	0.17	-0.19

BV parameters and adding Ewald and repulsive energy terms are essential for extending the model to calculate finite-temperature properties of larger DFT-inaccessible systems. We have employed SA techniques to optimize BV parameters to match DFT forces. Our preliminary investigations have shown that for the sample PT case reasonable agreement (average deviation of 0.032 eV/Å per coordinate) can be achieved. Furthermore, optimization of the BV parameters gives cohesive energies in agreement with DFT.

Future work on this empirical model will seek to investigate the size of the DFT database required to give BV parameters that give accurate forces for any structure. Also, more efficient minimization routines will be examined for the fine tuning of these parameters. An optimized BV model can be further adapted to MD simulations to investigate temperature-dependent properties for PT and other complex-oxide systems.

ACKNOWLEDGMENTS

This work was supported by the Office of Naval Research under grant number N-000014-00-1-0372 and through the Center for Piezoelectrics by Design. Computational support was provided by the High-Performance Computing Modernization Office of the Department of Defense and the Center for Piezoelectrics by Design. AMR would also like to thank the Camille and Henry Dreyfus Foundation for support.

REFERENCES

1. Brese, N., and O'Keefe, M., *Acta. Crystallogr.*, **47**, 192–197 (1991).
2. Brown, I. D., *Sturcture and Bonding in Crystals II*, Academic, New York, 1981, pp. 1–30.
3. Kohn, W., and Sham, L. J., *Physical Review*, **140**, A1133–A1138 (1965).
4. Ghosez, P., Cocakayne, E., Waghmare, U., and Rabe, K. M., *Physical Review B*, **60**, 836–843 (1999).
5. Huff, N. T., Demiralp, E., Cagin, T., and Goddard III, W. A., *Journal of Non-Crystalline Solids*, **253**, 133–142 (1999).

6. Bellaiche, L., and Vanderbilt, D., *Physical Review Letters*, **81**, 1318–1321 (1998).
7. Sepilarsky, M., Phillpot, S. R., Wolf, D., Stachiotti, M. G., and Migoni, R. L., *Applied Physical Letters*, **76**, 3986–3988 (2000).
8. Mercurio, D., Champarnaud, J. C., Gouby, I., and Frit, B., *European Journal of Solid State and Inorganic Chemistry*, **35**, 49–65 (1998).
9. Cooper, M. A., Hawthorne, F. C., and Grew, E. S., *Canadian Mineralogist*, **36**, 1305–1310 (1998).
10. Sawa, H., Ninomiya, E., Ohama, T., Nakao, H., Ohwada, K., Murakami, Y., Fujii, Y., Noda, Y., Isobe, M., and Ueda, Y., *Journal of the Physical Society of Japan*, **71**, 385–388 (2002).
11. Eck, B., and Dronskowski, R., *Journal of Alloys and Compounds*, **338**, 136–141 (2002).
12. Eck, B., Kurtulus, Y., Offermans, W., and Dronskowski, R., *Journal of Alloys and Compounds*, **338**, 142–152 (2002).
13. Adams, S., and Swenson, J., *Physical Review Letters*, **84**, 4144–4147 (2000).
14. Adams, S., and Swenson, J., *Physical Review B*, **63**, 0524201–1–054201–11 (2001).
15. Grinberg, I., Cooper, V. R., and Rappe, A. M., *Nature*, **419**, 909–911 (2002).
16. Dmowski, W., Egami, T., Farber, L., and Davies, P. K., "Structure of Pb(Zr, Ti)O_3 near the morphotropic phase boundary," in *Fundamental Physics of Ferroelectrics - Eleventh Williamsburg Ferroelectrics Workshop*, edited by R. E. Cohen, AIP, Woodbury, New York, 2001.
17. Press, W. H., Teukolsky, S. A., Vetterling, W. T., and Flannery, B. P., *Numerical Recipes in C: The Art of Scientific Computing*, Cambridge University Press, New York, 1997, pp. 444–451.
18. Metropolis, N., Rosenbluth, A., Rosenbluth, M., Teller, A., and Teller, M., *Journal of Chemical Physics*, **21**, 1087–1092 (1953).